Spontaneous formation of pH-sensitive, stable vesicles in aqueous solution of *N*-[4-n-octyloxybenzoyl]-L-histidine†

Trilochan Patra, Sampad Ghosh and Joykrishna Dey*

Received 14th January 2010, Accepted 19th April 2010
DOI: 10.1039/c000898b

A new amino acid-derived surfactant, sodium *N*-(4-n-octyloxybenzoyl)-L-histidinate (SOBH), was synthesized. The self-assembly properties and microstructure formation of SOBH was investigated by use of a number of techniques, such as surface tension, fluorescence spectroscopy, conductivity, dynamic light scattering (DLS), confocal fluorescence microscopy (CFM), and transmission electron microscopy (TEM). The amphiphile exists in both anionic and zwitterionic forms depending upon the pH of the solution and has very low critical aggregation concentration (CAC). The results of fluorescence probe studies and TEM as well as CFM pictures showed formation of vesicles in solution of pH > 7.5. The mean size and size distribution of the vesicles was measured by the DLS technique. The interaction of the amphiphile with cholesterol was also examined. In the presence of cholesterol the vesicle size and stability was observed to increase. Effects of salt, surfactant concentration, and temperature on the vesicle formation were investigated with or without varying amounts of cholesterol. Fluorescence anisotropy data indicated that the packing in bilayers becomes tighter by inclusion of cholesterol, which increased the stability of vesicles. The vesicles formed by SOBH were also found to be stable at body temperature.

Introduction

Colloidal self-assemblies composed of *N*-acyl-amino acid surfactants (NAAS) are a suitable model system for investigating several phenomena of interest to chemists and biologists because they are mild, non-irritating to human skin and highly bio-friendly. For these reasons they are commonly used as detergents and foaming agents, as well as in shampoos, cosmetics, paints, coating materials, drug formulation, drug and gene delivery and for oil extraction. For example, micelles,[1,2] vesicles,[3,4] or fibers,[5] that are sensitive to changes in pH, salt, temperature, or UV light could be potentially used as templates for materials synthesis,[6] or drug carriers and delivery devices.[7] Of particular interest are pH-sensitive vesicles, whose closed bilayer structure as well as hydrophilic core allows for the encapsulation and targeted release of drug and DNA molecules.[8] Hence, depending on the application, efforts have been directed toward the formulation of vesicles that are responsive to changes in pH. There are a few reports in the recent literature that describe pH-responsive vesicle formation by some amphiphilic molecules. Usually a bilayer of the pH-responsive vesicles/liposomes contains pH-sensitive amphiphiles having ionisable acidic, amine, imino or hydroxyl groups. For example, the pH-responsive character of the vesicles formed by amino acid-based amphiphiles,[9–11] phosphate group-containing amphiphiles,[12] sugar-based gemini surfactants,[13] fatty-acid-based amphiphiles,[14] alkyl amine oxides,[15] *N*-stearoylcysteamine,[16] *N*-palmitoyl homocysteine,[17] cholesteryl hemisuccinate,[18] sodium cholate,[19] fatty acid with phosphatidylethanolamine,[20] diacylsuccinylglycerols[20] and tocopherol hemisuccinate[21] have been reported. In these systems and in some cases like ion-pair amphiphiles, the pH sensitivity depends on charge as well as the chain length of the amphiphiles[22] which have the ability to destabilize the lipid bilayer when exposed to changes in the pH environment. The pH-induced vesicle-to-micelle transition has potential applications in drug delivery.[19,23–25] Di Marzio *et al.* showed the surfactant vesicle pH-sensitivity and cytoplasmatic delivery of drugs to target cells.[18,26] Some amphiphilic pH-sensitive vesicles are used for the controlled release of trapped materials from the inner aqueous core of the vesicle.[27,28] Similarly, vesicles which respond to the endosomal pH range are mostly used for efficient gene transfection.[29–31] Recently Dowling *et al.* created a vesicle-loaded gel to show the pH sensitivity.[32]

Derivatives of histidine are unusual surfactants in that the hydrophilic portion of the molecule is relatively large and contains both an anionic group (COO^-) and a cationic group (imidazole side chain), which gives this molecule an amphoteric nature by protonation-deprotonation to exhibit physicochemical behavior which is not typical of that exhibited by most NAAS.[33] Derivatives of histidine that respond to local pH changes in the body are helpful for solid tumor treatment.[2] Cationic amphiphiles containing histidine functionalities in their head group are serum compatible, nontoxic and endosome-disrupting, thus they can be used as a synthetic nonviral gene carrier.[34] In some cases amphiphiles of histidine also form translucent gels, fibrous structures or helical rods either in water or in water–ethanol mixtures.[35,36] The stereoselective deacylation of long-chain amino acid esters by chiral co-micelles of *N*-acyl-L-histidine and various cationic surfactants has been reported.[37] Antioxidant activity toward lipid peroxidation and the excellent emulsifying

Department of Chemistry, Indian Institute of Technology, Kharagpur, 721 302, India. E-mail: joydey@chem.iitkgp.ernet.in; Fax: +91-3222-255303; Tel: +91-3222-283308

† Electronic supplementary information (ESI) available: Optical microscope images and size distribution profiles of the aggregates. See DOI: 10.1039/c000898b

activity of *N*-acyl-L-histidine have also been reported.[38] This attracted our attention toward the self-assembly properties of histidine-containing amphiphiles. Recently, we have shown that 4-(*N*-n-alkyloxybenzoyl)-L-histidine amphiphiles produce thermoreversible, pH-responsive hydrogels in buffered water at different pH.[39]

In this work, we have investigated the aggregation behavior of sodium 4-(*N*-octyloxybenzoyl)-L-histidinate (SOBH) in dilute aqueous solutions. Earlier work in our laboratory has shown that this group of amphiphiles, with an amino acid head group, spontaneously forms vesicles and chiral helical aggregates in water.[3,40] However, vesicles formed by these amphiphiles were observed to be unstable in concentrated solution, in the presence of salt, and with a pH change. In order to prepare pH-responsive stable vesicles, we have studied the self-assembly properties of SOBH in aqueous solution. The major objectives of this study are (i) to characterize the aggregates formed by SOBH in aqueous solution, (ii) to investigate the effect of pH, salt concentration, and temperature on the self-assembly formation of SOBH, and (iii) to examine vesicle and chiral aggregate formation in aqueous solution. In this report, we also present the results of physical changes in membranes induced by mixing of SOBH with cholesterol by fluorescence anisotropy using 1,6-diphenylhexatriene as the probe molecule. We have used various techniques, such as surface tension, conductivity, fluorescence, dynamic light scattering, confocal fluorescence microscopy (CFM), and transmission electron microscopy (TEM) to characterize the system.

Experimental section

Materials

4-Hydroxybenzoicacid, 1-bromooctane, and anhydrous potassium carbonate, sodium bicarbonate, N-hydroxysuccinimide (NHS), 1,3-dicyclohexylcarbodiimide (DCC), L-histidine were purchased from SRL, Mumbai, India and was used without further purification. The fluorescence probes 5(6)-carboxyfluorescein (CF), pyrene, and 1,6-diphenyl-1,3,5-hexatriene (DPH) were obtained from Aldrich (Milwaukee, WI, USA) and were purified by repeated recrystallization from an ethanol-acetone mixture. Cholesterol was also obtained from Aldrich. Analytical grade sodium hydroxide, and hydrochloric acid were procured locally and were used directly from the bottle. All the organic solvents were of good quality and commercially available and were dried and distilled fresh before use. Double distilled water was used for the preparation of aqueous solutions.

Synthesis

N-[4-n-octyloxybenzoyl]-L-histidine was synthesized according to the procedure described elsewhere.[41,42] Briefly, 4-octyloxybenzoic acid was first synthesized from 4-hydroxybenzoic acid and 1-bromooctane and purified according to the reported procedure.[43] The coupling of L-histidine and 4-octyloxybenzoic acid was made *via* the formation of the NHS ester in the presence of DCC in THF–H_2O medium. The product was precipitated out from aqueous solution at around pH 4–5 and, the compound was purified by recrystallization from the ethanol–water mixture. The sodium salt of the compound (SOBH) was obtained by reacting *N*-[4-n-octyloxybenzoyl]-L-histidine with sodium methoxide in methanol and finally recrystallized from the acetone–water mixture. Chemical identification of the compound was performed by use of ^{1}H NMR and FT-IR spectroscopy.

Identification of chemical structures of SOBH

Yield 65%, M.P. 145–147 °C (d). $[\alpha]_D^{25}$ (0.5%, CH_3OH) = 6.80°, **FT-IR** (KBr, cm^{-1}): 3398,3304,3155, 2925, 2853, 1718, 1637, 1538, 1508,1400,1313,1250. **^{1}H-NMR:** δ_H (400 MHz, CD_3OD): 7.7 (2H, d, J8.8, Ph-*H*), 6.9 (2H, d, J8.8, Ph-*H*), 7.95 (1H, d, J8.8, N*H*), 8.49 (1H, S, CCHN), 7.2 (1H, S, NCHN), 4.72 (1H, dd, $J_1$5.2, $J_2$5.2, C*H*(NH)COOH), 4.0 (2H, t, J6.5, O–CH_2), 3.33 (2H, dd,J7.6 C*H*CH_2), 1.8 (2H, m, CH_2-CH_2–O), 1.47(2H, m, CH_2-CH_2-CH_2–O),1.32 (8H, m, alkyl chain), 0.9 (3H, t, J6.4, CH_3). **^{13}C-NMR:** δ_C (400 MHz, CD_3OD) 174.6 (*C*OOH), 167.6 (*C*ONH), 162.1, 128.7, 116.7, 113.6 (Ph-*C*), 133.3,131.3,125.6 (Im. ring -C), 67.7 (*C*H_2OPh), 53.7, 31.5 (valine *C*), 29.0, 28.9, 28.8, 27.9, 25.6, 22.2, 12.9 (R).

Methods and instrumentation

The FT-IR spectra were measured with a Perkin-Elmer (Model Spectrum Rx I) spectrometer. The ^{1}H NMR spectra were recorded on a Bruker 400 MHz instrument. The melting point measurement was done using Instind (Kolkata) melting point apparatus with open capillaries. A digital pH meter (Model PH 5652, EC India Ltd, Kolkata) was used for pH measurements. Conductivity was measured with a Thermo Orion conductivity meter (model 150 A+) by use of a cell having a cell constant equal to 0.467 cm^{-1}. The measurements of optical rotations were performed with a JASCO (Model P-1020) digital polarimeter. All measurements were done at room temperature (~30 °C) unless otherwise mentioned.

Surface tension measurements were carried out with a surface tensiometer (model 3S, GBX, France) using the Du Nuöy ring detachment method. The Pt–Ir ring was carefully cleaned with 50% ethanol–HCl solution and finally with distilled water. The ring was carefully flamed before measurement. The glassware was thoroughly cleaned with sulfochromic acid and water. The instrument was calibrated and checked by measuring the surface tension of distilled water. A stock solution of surfactant was made in double distilled water. An aliquot of this solution was transferred to a beaker containing a known volume of buffer solution. The solution was gently stirred magnetically through a magnetic stirrer attached with the machine and allowed to stand for about 5 min. The temperature of the solution was controlled at 30 °C by a thermostat, and then surface tension was measured. For each measurement at least three readings were taken and the mean γ value was recorded.

In the absence of cholesterol vesicles were formed spontaneously when SOBH was dissolved in different pH. Separate solutions of SOBH in the presence of varying amount of cholesterol were made by adding different mole ratios of the surfactant (SOBH) in methanol and cholesterol in chloroform and were evaporated to dryness in glass vials under a stream of dry nitrogen gas and were kept under high vacuum overnight for complete removal of the last trace of organic solvent. The

surfactant/cholesterol mixtures were dispersed in a phosphate buffer of appropriate pH for 4 h at room temperature. Finally the dispersion thus obtained was sonicated individually for 2–5 min to give the resulting solution.

The UV-visible spectra were recorded on a JASCO (Model V-530, Japan) spectrophotometer. Fluorescence spectra of the pyrene probe ($\sim 2 \times 10^{-7}$ M) were measured with a SPEX Fluorolog-3 spectrofluorometer. The samples were excited at 335 nm and the emission spectrum was recorded between 350 and 450 nm. The steady-state fluorescence anisotropy of DPH was measured on a Perkin Elmer LS-55 luminescence spectrometer equipped with filter polarizers that used the L-format configuration. The software supplied by the manufacturer automatically determined the correction factor and anisotropy value. The *r*-value was calculated employing the following equation:

$$r = (I_{VV} - GI_{VH})/(I_{VV} + 2GI_{VH}) \quad (1)$$

where I_{VV} and I_{VH} are the fluorescence intensities polarized parallel and perpendicular to the excitation light, and $G\,(= I_{HV}/I_{HH})$ is the instrumental grating factor. In all cases, the anisotropy values were averaged over an integration time of 10 s and a maximum number of five measurements for each sample. The temperature of the water-jacketed cell holder was controlled by use of a Thermo Neslab RTE 7 circulating bath. Since DPH is insoluble in water, a 0.5 mM stock solution of the probe in methanol was prepared. The final concentration of the probe was adjusted to 1.0 μM by addition of an appropriate amount of the stock solution. The sample was excited at 350 nm and the emission intensity was followed at 450 nm using excitation and emission slits with band-pass of 2.5 and 2.5–7.0 nm, respectively. A 430 nm emission cut-off filter was used to reduce scattered and stray radiation. All fluorescence measurements were carried out at 30 ± 0.1 °C. The measurements started 2–3 h after sample preparation.

Time-resolved fluorescence measurements were performed on a time-correlated single-photon counting method that uses a picosecond diode laser at 370 nm (IBH, U.K., nanoLED-07) as a light source. The typical response time of this laser system was 70 ps. Fluorescence lifetimes were determined from time-resolved intensity decay by the method of time-correlated single-photon counting. The decays were analyzed using IBH DAS-6 decay analysis software. For all the lifetime measurements the fluorescence decay curves were analyzed by a biexponential or triexponential iterative fitting program provided by IBH.

The dynamic light scattering (DLS) measurements were performed with a Zetasizer Nano ZS (Malvern Instrument Lab, Malvern, U.K.) optical system equipped with a He–Ne laser operated at 4 mW at $\lambda_o = 633$ nm, and a digital correlator. Before measurement, the scattering cell was rinsed several times with the filtered solution. The DLS measurements started 5–10 min after the sample solutions were placed in the DLS optical system to allow the sample to equilibrate at room temperature. For all light-scattering measurements, the temperature was 30 °C. The scattering intensity was measured at a 173° angle to the incident beam. The data acquisition was carried out for 10 min and each experiment was repeated two or three times. The data were analyzed using the second-order cumulant method.[44] The time decay of the autocorrelation function of the concentration fluctuations has a characteristic decay rate, Γ, which is proportional to q^2 ($\Gamma = Dq^2$) that characterizes a translational diffusion with the mutual diffusion constant, D. The scattering vector, q, is given by the equation:

$$q = 4\pi n/\lambda_0 \sin(\theta/2) \quad (2)$$

where n is the refractive index of the solvent, and θ is the scattering angle. The measured translational diffusion constant was related to the average hydrodynamic radius, R_H, of the particles through the equation:

$$D = kT/6\pi\eta R_H \quad (3)$$

where k is the Boltzmann constant, η the solvent viscosity, and T the absolute temperature.

The samples for high resolution transmission electron microscopic measurements were prepared according to the usual procedure, described as follows. A 5 μL of the surfactant solution was placed on the 400 mesh carbon-coated copper grid, blotted with filter paper, and negatively stained with freshly prepared 1.5% phosphotungstate after adjustment of pH to the solution pH. The specimens were dried overnight in desiccators before measurement with a high resolution transmission electron microscope, HRTEM (JEOL-JEM 2100, Japan) operating at 200 kV.

The optical light micrographs for the samples were obtained from a Leica-DM4500 optical microscope. Confocal fluorescence microscopic images were obtained with a FV 1000 Olympus Confocal Microscope with PLAPON 60 X oil immersion objectives. The numerical aperture was 1.42, a 488 nm laser was used as the excitation source. The fluorescence was viewed using a 520 nm filter. The image was processed using FV10-ASW 1.6 viewer software. For fluorescence microscopy, CF was trapped into the vesicle by gentle mixing of the surfactant (1 mM for pH 8 and 8 mM for pH 12) and CF (1 mM) into methanol and followed by rotary evaporation. The dry film thus produced was soaked overnight in buffer of appropriate pH, vortexed and sonicated for 5 min. The aqueous solution was obtained after appropriate dilution. The excess dye was removed by dialysis for 10–12 h using an ultrafiltration cellulose acetate membrane bag (16 mm diameter, 10 kDa MWCO). An aliquot of the undiluted vesicle solution was pipetted onto the glass slide and sealed with a coverslip and left to sit the coverslip down for a few minutes before analysis.

Results and discussion

Ionization behavior in solution

To our surprise, it was found that the amphiphile (SOBH) has very low solubility in water in the pH range 3–7 at room temperature. The pK_a values corresponding to the protonation of COO^- and dissociation of -NH^+ imidazole groups for histidine are 1.77 and 6.1, respectively.[45] But for long chain amphiphiles the pK_a values are usually higher.[46] Indeed, the pK_a values of N^{α}-octadecanoyl-L-histidine at 25 °C, as reported by Kashima *et al.* are 3.12 (COOH) and 7.49 (NH^+).[46b] Thus, SOBH is also expected to have similar pK_a values. Consequently, it was

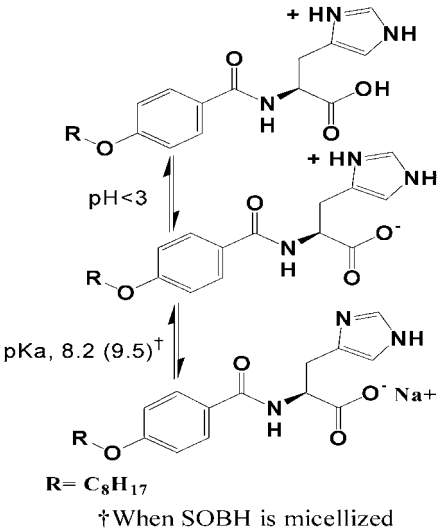

Scheme 1 The proton transfer equilibria in aqueous solution of SOBH.

observed to become soluble in water at pH>7 as it transformed into the anionic form. But below pH 3.0 it forms a turbid solution. Therefore, the aggregation behavior of the amphiphiles was studied at pH 8.0 and 12 where it exists mostly in the zwitterionic and anionic form, respectively, as shown in Scheme 1.

Surface tension studies

The critical aggregation concentration (CAC) of the chiral surfactants was measured by the surface tension (ST) method, which is versatile not only because CAC can be extracted from the plots of surface tension (γ) *versus* log[Surfactant] but also information can be drawn on the nature of adsorbed layers at the air/water interface. The typical plots of surface tension *versus* log *C* (logarithmic value of surfactant concentration) for an aqueous solution at pH 8.0 and 12.0 of the surfactants are shown in Fig. 1. The surface tension values decrease linearly with log *C* and show a characteristic break and remain constant thereafter. In pH 8.0 the plot shows a hump, which represents the presence of two forms of molecule, one is in anionic form and another in zwitterionic form. The concentration corresponding to the breakpoint was taken as the CAC value. The surface-active

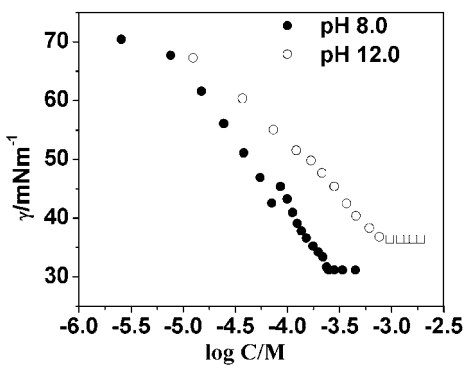

Fig. 1 A plot of surface tension (γ) *vs.* log *C* of SOBH in 20 mM phosphate buffer at pH 8.0 and 12.0 at 30 °C.

Table 1 The self-assembly properties of SOBH in 20 mM phosphate buffer of pH 8.0 and pH 12.0 at 30 °C

Properties of SOBH	pH = 8.0	pH = 12.0
CAC (mM)	0.26	0.84
γ_{CAC}/mN m^{-1}	31.0	36.4
pC_{20}	4.42	3.90
$\Gamma_{max} \times 10^6$ (mol m^{-2})	2.0	1.83
A_{min} (Å^2 molecule^{-1})	41.0	45.0
P	0.66	0.60
I_1/I_3	1.11	1.38
η_m (mPa s)	55.8	46.2 (22.3)[a]

[a] The value within the parentheses was obtained using 8.0 mM SOBH at pH 12.0.

parameters, such as CAC, surface tension corresponding to CAC (γ_{CAC}), and efficiency of adsorption, pC_{20} (= negative logarithm of surfactant concentration required to reduce the γ of water by 20 units) were determined from the ST plot for SOBH at pH 8.0 and 12.0. All the physicochemical parameters are listed in Table 1.

The values of the surface excess (Γ_{max}) and cross-sectional area per head-group (A_{min}) at the air/water interface were calculated by using the Gibbs adsorption equations,[47,48]

$$G_{max} = -1/2.303nRT\,(d\gamma/d\log C) \quad (4)$$

$$A_{min} = 1/N_A\,\Gamma_{max} \quad (5)$$

where $d\gamma/d\log C$ is the maximum slope; N_A is Avogadro's number; T = absolute temperature; n = 1 for a 1 : 1 ionic surfactant in the presence of a swamping amount of 1 : 1 electrolyte;[47] R = 8.314 J mol^{-1} K^{-1}. The cross-sectional areas were calculated from Γ_{max} values corresponding to the break of the ST plot (Fig. 1). It should be noted that SOBH has a slightly lower A_{min} value (Table 1) at pH 8.0 than at pH 12.0. The smaller value of A_{min} at both pH suggests the formation of large aggregates with tightly packed hydrocarbon chains. This is further indicated by the critical packing parameter, P (= $v/A_o l$, where A_o is the area per headgroup in the aggregate, v and l are the volume and length of the hydrophobic chain, respectively)[49] of the species at the above pH values. With reasonable accuracy, P can be equated to $v/A_{min}l$.[50] The value of v (0.419 nm^3) was calculated using the atomic increment method after appropriate correction.[51] On the other hand, the value of l (1.54 nm) was calculated as the fully stretched chain of the energy minimized (MM2) structure using Chem3D (version 5.0) program. The P values thus obtained have been included in Table 1. The large values of P (>0.5) at both pH are indicative of the existence of bilayer structure.[49] The formation of spherical bilayer vesicles for this class of amphiphiles in dilute solution is due to intermolecular hydrogen bonding (IHB) between amide groups and π–π stacking interaction between benzene rings and the close packing of the hydrocarbon tails which has been reported earlier[3,40,42] and has been substantiated by the results of fluorescence probe studies discussed below.

We have also measured the CAC value of SOBH in different pH solutions using the ST method. Variation of CAC as a function of pH is shown by the plot in Fig. 2. It can be found that CAC increases with pH reaching a plateau at pH>11, which must

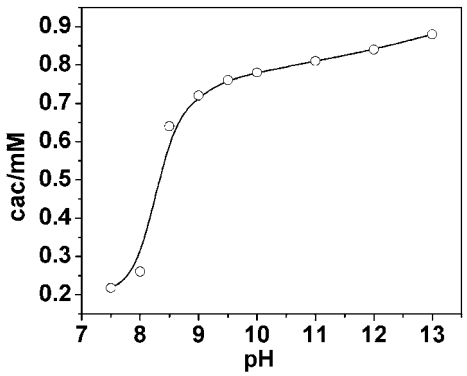

Fig. 2 The variation of the CAC of SOBH with pH in 20 mM phosphate buffer at 30 °C.

be due to the gradual conversion of the zwitterionic species to anionic species at higher pH. Increased ionic repulsion among surfactant headgroups at pH>11 decreases hydrophobic interaction and thus increases CAC value. The pH (*ca.* 8.2) corresponding to the inflection point of the curve can be taken as the macroscopic pK_a of the NH^+ group of the imidazole ring. It is interesting to note that the pK_a of the NH^+ group of SOBH is higher than that of N^{α}-octadecanoyl-L-histidine.[46(b)]

Fluorescence probe studies

In order to understand the pH dependent structural change of the surfactant aggregates, we have performed steady-state fluorescence anisotropy (r) measurements. The r is an index of equivalent microviscosity in the vesicle lipidic core. The DPH is a well-known membrane fluidity probe.[52] Therefore, the r-value of DPH was measured in different buffer solutions in the pH-range of 8–12. The r-value is relatively high for lower pH (~8.0), which decreases with an increase in pH as shown by the plot in Fig. 3. The relatively high values of r in pH 8.0 and 12.0 suggest an ordered environment around the DPH probe in the self-assemblies and thus supports the existence of bilayer structures.[3,40,42,53] The results are thus consistent with those obtained by ST studies. Slightly lower values of r in pH 12.0 (~0.16) is due to the electrostatic repulsion among headgroups in the aggregate that weakens the hydrophobic interaction of the hydrocarbon chains. However, the presence of the bulky imidazole ring reduces the electrostatic repulsion among the

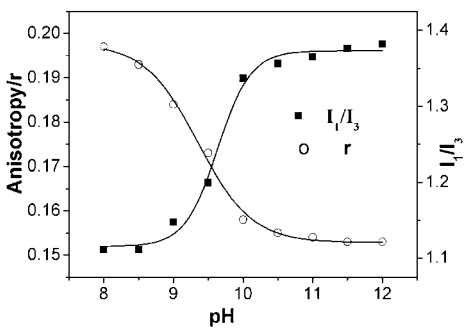

Fig. 3 A plot of r and I_1/I_3 against pH in the presence of 1.5 mM SOBH at 30 °C.

negatively charged headgroups, which favors the formation of bilayer aggregates in dilute solution. Consequently, the packing of the hydrocarbon chains becomes less tight compared to the bilayer aggregates in pH 8.0, which allows more water molecules to penetrate into the hydrocarbon core of the aggregate. This means an increase of both fluidity and polarity of the microenvironments of probe molecules.

In order to quantify the rigidity of the hydrocarbon chain of the aggregates formed in pH 8.0 and 12.0, we have determined microviscosity around the DPH probe in the surfactant aggregate. The microviscosity (η_m) can be calculated from the Debye-Stokes-Einstein relation[54,55] using the r-value and fluorescence lifetime (τ_f) of the DPH molecule in the presence of surfactant according to the procedure described in the literature.[56] The τ_f values obtained from the analysis of fluorescence intensity decays of the DPH probe in the presence of the SOBH amphiphile at pH 8.0 and 12.0 are 5.39 ns, and 5.3 ns, respectively. The microviscosity values thus calculated are presented in Table 1. The η_m-value for the self-assemblies of SOBH at pH 12.0 at higher concentration (8.0 mM) is 22.32 mPa s, which is similar to those of micellar aggregates of SDS and DTAB surfactants.[56] However, at low surfactant concentration, the η_m-value for the self-assemblies at pH 8.0 (55.8 mPa s) and 12.0 (46.2 mPa s) are larger than that of ionic micelles.[56] The relatively higher η_m-value in a dilute solution of SOBH is consistent with the formation of bilayer aggregates. The lower values of η_m for the bilayer aggregates compared to liposomes is due to quenching (collisional) of fluorescence of the DPH molecule by the imidazole ring present in the head group of SOBH, which reduces the τ_f value. This was verified by a simple experiment. We made two solutions of sodium *N*-(4-n-octyloxybenzoyl)-L-valinate (SOBV) and SOBH having the same DPH and surfactant concentration. It was observed that the fluorescence intensity of DPH was quite low for the SOBH surfactant in comparison to SOBV[3] at room temperature. It should also be noted that the τ_f value of the DPH probe in SOBH (5.39 ns) is less than that observed in the SOBV (6.30 ns) solution. In fact, the ratio (1.14) of fluorescence intensity in SOBV to that in SOBH is almost equal to the ratio (1.16) of the corresponding fluorescence lifetimes, which suggests that the fluorescence quenching in the SOBH solution is dynamic in nature.

For bilayer aggregates, as discussed before, the packing of the hydrocarbon chains of the amphiphilic molecules in the aggregate is very tight compared to micellar aggregates (*e.g.* spherical or rod-like micelles). This means that the hydrocarbon region of the bilayer aggregates will be much less polar compared to micellar aggregates. The micropolarity of the self-assemblies formed in pH 8 and 12 was therefore measured by use of a pyrene probe whose fluorescence property is sensitive to polarity change. It is well known that the ratio of the intensities of the first and third vibronic bands (I_1/I_3) in the fluorescence spectrum of pyrene is sensitive to solvent polarity change.[57,58] Therefore, this parameter was used to test changes in the micropolarity of the aggregates upon change of solution pH. The data are plotted against pH in Fig. 3. The I_1/I_3 value for the SOBH amphiphile measured at a concentration around two times its CAC value is much less than that in the pH 12.0 buffer (1.80), indicating solubilization of the pyrene molecule in the hydrophobic region of the aggregate. However, it is interesting to observe that the

I_1/I_3 index decreases further with the decrease of pH (Fig. 3) indicating a decrease of micropolarity. This is consistent with the decrease of membrane rigidity (η_m) of the bilayer self-assembly with the increase of pH as indicated by the decrease of fluorescence anisotropy (r) of DPH with the increase of pH. This must be a consequence of the transformations of SOBH from zwitterionic to anionic form which results in an increase of electrostatic repulsion among headgroups, thus allowing penetration of more water molecules into the bilayer and thereby increaseing the micropolarity parameter. This means leakage of entrapped drugs, if any, can be facilitated by increase of the pH. In other words, controlled release of drugs can be achieved.

It is important to note that the pK_a value of the imidazole nitrogen as obtained from the titration curves in Fig. 3 is *ca.* 9.5 which is higher than the macroscopic pK_a (~8.2) value of SOBH. This must be due to aggregate formation. Such aggregation induced pK_a shift has also been noted by others.[59] The higher pK_a value for the long chain amphiphilic molecule is because the local pH value at the surface of the negatively charged aggregate is lower than the pH of the bulk solution.

In order to investigate the concentration dependent aggregation behavior of SOBH, we also measured the fluorescence anisotropy of the DPH probe at different concentrations in pH 12. The result is presented in Fig. 4, which shows that the r-value continuously decreases with the increase of [SOBH] up to 12 mM and thereafter remains unchanged. In light of the above discussion, the low r-value in concentrated solution can be associated with the formation of rod-like micelles. Such studies in pH 8 could not be done at room temperature because of precipitation of SOBH at concentrations higher than 1.0 mM. Due to strong electrostatic attraction the large aggregates that are formed at higher concentration fall out of solution.

Conductivity measurements

To examine the shape of the bilayer structures formed in pH 12 buffers we performed conductivity measurements. Closed vesicular structures can be confirmed from conductivity measurements of the vesicular solution in the presence of KCl. Bilayer aggregates, such as vesicles, entrap a part of the water and the salt present in it. Consequently the entrapped charge carrier ions are prevented from contributing to the conductivity of the solution, which means a decrease of the conductivity of the vesicular solution. In fact, the decrease of electrical conductivity

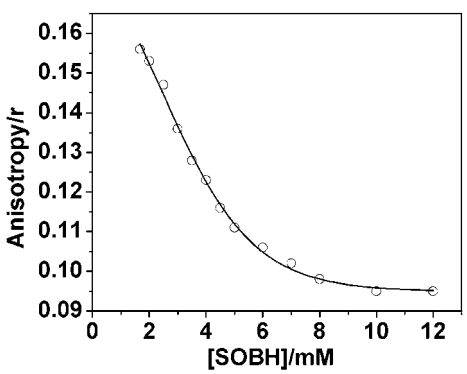

Fig. 4 A plot of r of DPH against [SOBH] in pH 12.0 buffer at 30 °C.

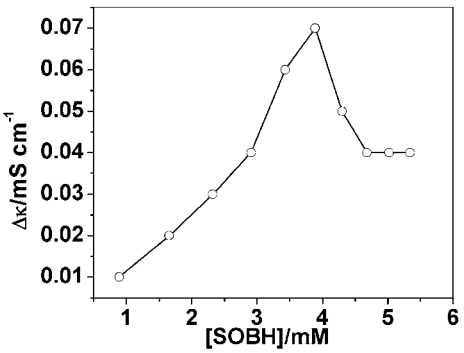

Fig. 5 The characteristic specific conductance change ($\Delta\kappa$) *vs.* [SOBH] in the presence of 3 mM KCl in phosphate buffer of pH 12.0 at 30 °C.

of salt solution upon addition of vesicle-forming surfactants has also been reported by others.[60] The conductivity of a 3 mM KCl in the presence of different concentrations of the surfactant was measured at 30 °C. It was observed that the sum of the conductivities of the solutions of 3 mM KCl and 1 mM SOBH (20 mM phosphate buffer pH 12.0) was greater than that of 1 mM SOBH (20 mM phosphate buffer pH 12.0) containing 3 mM KCl. This means that the conductivity of the KCl solution is decreased in the presence of 1 mM (>CAC_1) SOBH. The variation of conductivity change ($\Delta\kappa$) with the increase of [SOBH] is shown in Fig. 5. It can be observed that although the initial value of $\Delta\kappa$ is small, it increases nonlinearly with surfactant concentration. The $\Delta\kappa$ value reaches a maximum at around 4 mM and then drops down at [SOBH]>4 mM. This is clear evidence of the formation of vesicles that have an aqueous core in concentrations up to 4 mM in pH 12.0. Since both size and population of vesicles increases with surfactant concentration, more K^+ and Cl^- ions get trapped inside the aqueous core and hence display an increase in the $\Delta\kappa$ value. The fall of the $\Delta\kappa$ value above 4 mM is perhaps due to transformation of vesicles to other kind of aggregate structures that lack aqueous core like vesicles.[61] Indeed as suggested by the concentration dependence of fluorescence anisotropy of the DPH probe the vesicles are transformed into rod-like micelles. That the release of the entrapped water and ions occurs at a high surfactant concentration is supported by the lowering of the fluorescence anisotropy of the DPH probe (see Fig. 4).

Transmission electron microscopy (TEM)

To further visualize the shape of the surfactant aggregates in solution we obtained TEM pictures of negatively stained samples of the dilute solutions of SOBH at pH 8.0 and pH 12.0 (Fig. 6(a)–(c)). The images in Fig. 6(a) and 6(b) clearly reveal the existence of spherical vesicles with an aqueous cavity. This supports the results obtained from the ST, fluorescence, and conductivity studies. The inner diameters of the vesicles are in the range 30–100 nm. The formation of smaller size vesicles of around 30–50 nm diameter in dilute aqueous solutions of pH 8 is due to the presence of the mostly zwitterionic form of the amphiphiles. The image in Fig. 6(c) taken for a 10 mM solution in pH 12.0 reveals a bunch with rod-like morphology. These are a few micrometres long and have very small inner diameter. The transition from

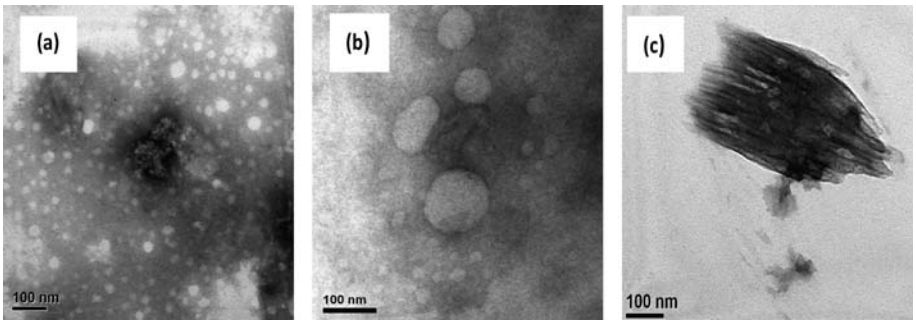

Fig. 6 Negatively stained (sodium phosphotungstate) transmission electron microscopic images of aqueous SOBH: (a) 0.5 mM, pH 8.0, (b) 2.0 mM, pH 12.0, and (c) 10 mM, pH 12.

vesicle to rod-like micelles at higher surfactant concentration has been previously reported by us.[62] The transformation of vesicles to rod-like structures is consistent with the decrease in fluorescence anisotropy (see Fig. 4) of the DPH probe and specific conductance (see Fig. 5) of KCl salt with the rise of surfactant concentration above 4 mM. In fact, the appearance of fiber-like aggregates was observed upon standing of the sample for a few days. This can also be visualized in the optical micrographs shown in Fig. S2 of the ESI†. The micrograph (b) of Fig. S2† also reveals the existence of helical aggregates.

Confocal fluorescence microscopy

To further support the results obtained from TEM studies we have also performed confocal fluorescence microscopic measurements using dilute aqueous solutions of SOBH. The optical images (Fig. 7) obtained for samples in pH 8 and 12 exhibit vesicular structures. However, only large vesicles could be seen under the microscope. The smaller vesicles having a diameter of less than 100 nm could not be observed because of limited resolution of the microscope. The existence of vesicles in dilute solutions of both pHs is thus confirmed.

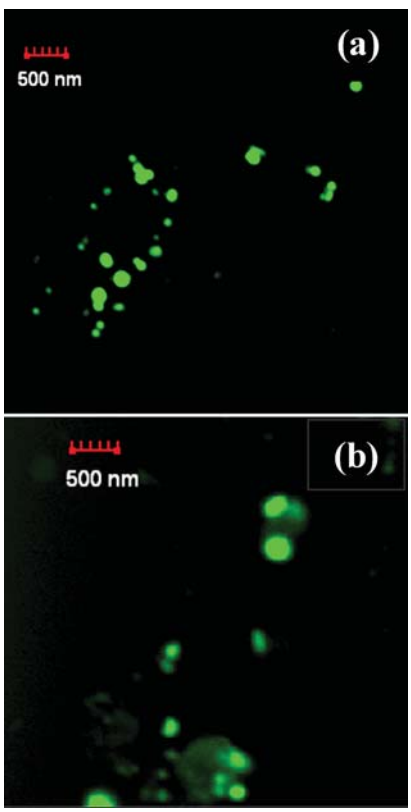

Fig. 7 Fluorescence microscopic images of aqueous SOBH: (a) 0.5 mM, pH 8.0, and (b) 2.0 mM, pH 12.0.

Hydrodynamic size of the aggregates

The mean hydrodynamic diameter (d_H) of the aggregates was measured by DLS technique at different concentrations and pH. The volume distribution graphs for the amphiphile are shown in Fig. 8. It is observed that the aggregates formed in pH 8 and 12 have narrow and bimodal size distributions. The aggregates are found to be much larger in size than small spherical micelles which have diameters typically in the range 3–5 nm.[63] The d_H values of the aggregates in 0.5 mM (pH 8) are found to be in the range of 30–200 nm, whereas those in 2.0 mM (pH 12) solution of SOBH the particle size is in the range 60–300 nm. In both pHs, the volume fraction of the larger size particles is much lower compared to the small size particles. However, the sizes of the small and large particles are closely equal to the vesicle structures observed in the corresponding TEM as well as optical micrographs. At higher SOBH concentration (8.0 mM, pH 12), the *z*-average d_H value is *ca.* 1.0 μm (this value is not correct because the principle involved in DLS measurements is only applicable for spherical particles) indicating the existence of large aggregates. This is consistent with the TEM picture (Fig. 6(c)) and can be attributed to the transformation of the small spherical vesicles to large rod-like micelles upon increase of surfactant concentration. The appearance of a small hump on the higher size range of the distribution in Fig. 8(c) perhaps indicates that large fibers separate out of solution with time. Indeed, the appearance of long fibrous aggregates could be observed even with naked eye when the concentration was increased further.

Influence of salt concentration

The influence of salt concentration and temperature on the stability of vesicle was investigated by monitoring the fluorescence anisotropy (*r*) of the DPH probe in surfactant solutions. In the presence of NaCl salt the *r*-value was observed to decrease. Fig. 9 shows the plot of the variation of *r* as a function of [NaCl] for a particular concentration of SOBH. It is observed that for

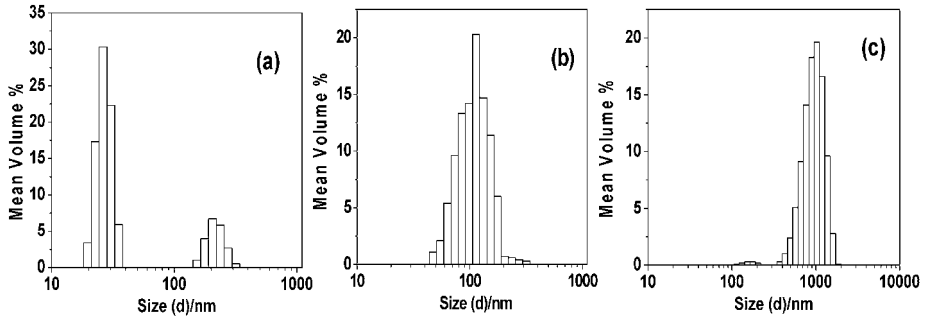

Fig. 8 The size distribution profile of aggregates in (a) 0.5 mM, pH 8.0, (b) 2.0 mM, pH 12, and (c) 10 mM, pH 12 SOBH solution.

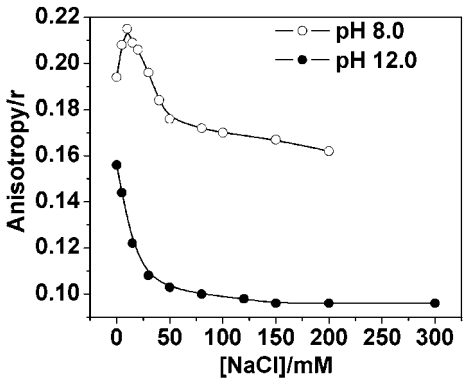

Fig. 9 A plot of fluorescence anisotropy (r) of DPH in the presence of 0.5 (pH 8) and 2.0 mM (pH 12) SOBH against [NaCl].

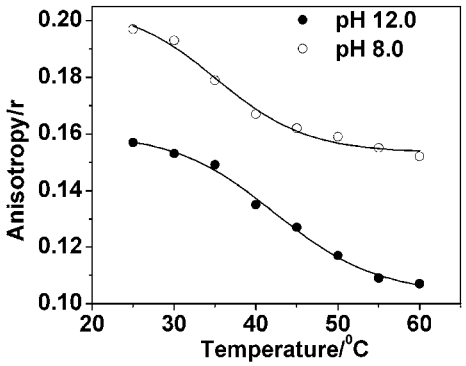

Fig. 10 A plot of fluorescence anisotropy (r) of DPH in the presence of 0.5 (pH 8) and 2.0 mM (pH 12) SOBH against temperature.

pH 8.0, the r-value initially increases, reaches a maximum at *ca.* 20 mM NaCl and then decreases with a further increase in salt concentration. But at pH 12.0, a sharp decrease of r-value can be observed, suggesting the transformation of the bilayer structure to rod-like micelles at a relatively low NaCl concentration (~20 mM). Similar behavior was also observed with a SOBV surfactant.[3] For the pH 8 solution, even in the presence of 200 mM NaCl, the r-value is not as low as it is observed with the pH 12 solution. The initial increase in r-value is due to the counter ion balance that facilitates growth of vesicles. The results indicate that the vesicles are quite stable under physiological conditions (pH 7.4, 150 mM NaCl). However, the decrease of membrane rigidity at higher salt concentrations suggests that NaCl can be used to induce slow release of encapsulated drugs.

Effect of temperature

It has been found that vesicles formed in different pH have different physical properties and stability.[10,64] For this we have also studied the stability of vesicles at different temperature in the range 20–60 °C. The temperature stability of vesicles was studied by use of a DPH probe. Fig. 10 shows the plots of the variation of r-value of DPH as a function of temperature for both pH 8 and 12 at a particular concentration of SOBH. The r-value is higher at low temperature, but it decreases with the rise in temperature. However, at 60 °C the r-value is much less for pH 12 and corresponds to micellar structure. On the other hand, for vesicle solutions at pH 8, the r-value is higher even at 60 °C and indicates the existence of vesicles. The decrease of r-value with the increase of temperature can be associated with the weakening of the hydrophobic interactions among hydrocarbon chains in the aggregate as a result of disruption of the intermolecular hydrogen bonds and other physical forces. This means that the hydrocarbon chains become more fluid at higher temperatures. In other words, a phase transition from a more ordered gel-like bilayer state to a slightly less ordered liquid-crystal state occurs in the pH 8 vesicle solution upon increase of temperature. However, in the pH 12 solution, the r-values in the initial and final states suggest that the phase transition occurs between vesicle and micellar states. Since the r-value decreases with the rise in temperature, the temperature corresponding to the inflection point can be taken as the melting or phase transition temperature, T_m of the vesicles. The high melting temperature, (~40 °C) for both pH 8 and 12 clearly suggests that the vesicles are quite stable at physiological temperature (37 °C).

Effects of cholesterol

Cholesterol (Chol) is known to impart rigidity to phospholipid membranes and thus control the permeability of cellular substances through membranes.[65] In order to study the interaction of Chol with the bilayer membranes formed by SOBH, we investigated the effect of adding increasing levels of Chol to SOBH solution at pH 8.0 and 12.0 and also the variation of SOBH concentration at fixed mole % of Chol through fluorescence anisotropy of the DPH molecule (Fig. 11(a) and (b)). Usually, there is an upper limit to Chol incorporation in lipid bilayers, above which Chol seems to precipitate as crystals of

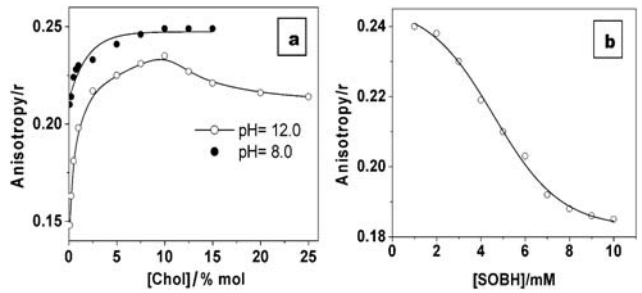

Fig. 11 A plot of the fluorescence anisotropy of DPH (a) as a function of mol% of Chol in 0.5 mM and 2.0 mM SOBH at pH 8.0 and 12.0, respectively, (b) against [SOBH] containing 10 mol% Chol at pH 12.0 at 30 °C.

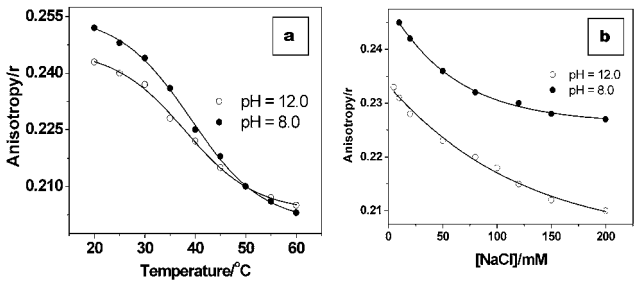

Fig. 12 A plot of fluorescence anisotropy of DPH *versus* (a) temperature and (b) [NaCl] in the presence of 0.5 and 2.0 mM SOBH containing 10 mol % Chol at pH 8.0 and pH 12.0, respectively.

pure Chol either in the monohydrate or in the anhydrous form.[66] Huang *et al.*[67] observed that for a membrane composed by phosphatidylcholine (PC) the maximum cholesterol solubility is about 66 mol% and by phosphatidylethanolamine (PE) the limit is about 51 mol%, depending on the acyl chain composition. As the concentration of Chol increases, the system undergoes a process of phase separation to form Chol-rich domains.[68] In our case, addition of *ca.*10 mol % Chol gave the highest fluorescence anisotropy value but at still higher mol% Chol, the *r*-value decreased. Interestingly, the decreases in anisotropy observed at the higher levels of Chol appeared to be accompanied by an increase in vesicle aggregation due to less solubilization of higher mol % Chol as evidenced by the appearance of turbidity. The growth of vesicles to larger sizes (perhaps due to the formation of multilamellar vesicles) is evidenced by the increase of mean hydrodynamic diameter (see size distributions in Fig. S2 of the ESI†). However, the latter effect may be due to the formation of Chol clusters at high Chol content where excess amounts of Chol cannot interact with the SOBH, and deposits on the bilayers.

We also found that the presence of 10 mol% Chol with increasing surfactant concentration at pH 12.0 keeps the anisotropy values higher than that of the pure surfactant solution. These anisotropy data provide some quantitative estimates on the fluidity of the interior of lipid vesicles and lipid-Chol co-aggregates. Results show that addition of Chol makes the bilayer membrane more rigid both in pH 8.0 and 12.0. This rigidity offers more stability to the vesicles, even at a higher concentration of surfactant, than the vesicles produced by pure SOBH. The plot in Fig. 11(b) shows a decrease of *r*-value with [SOBH] in SOBH-Chol mixture suggesting a concentration-dependent phase change in pH 12.0 even in the presence of 10 mol% Chol. However, a relatively large *r*-value at higher concentration indicates that the bilayer structure is still retained. The decrease of *r* may therefore be attributed to the transformation of closed bilayer vesicles to a flat lamellar structure which is evidenced by the large increase in the hydrodynamic diameter of the aggregates (see Figure S2 of the ESI†).

It is known that the presence of Chol is responsible for the orientation and packing of the lipid hydrophobic chain.[69] This hydrophobic association of the lipid and Chol imposes a restriction on the chain $(CH_2)_n$ motions,[70] and offers rigidity to the self-assembly. This in turn alters the thermotropic phase transition temperature in the lipid bilayer region of the membrane and also influences their permeability and stability to the external environment. In order to assess such behavior we have studied the effect of temperature, salt, and pH for vesicles formed from a SOBH-Chol (10%) mixture. The addition of 10 mol% Chol to lipids generally causes broadening of the phase transition process and hence distinct thermal phase transitions are not observed. The temperature effect on the vesicle stability formed from the SOBH-Chol (10%) mixture has been shown by the plots (Fig. 12(a)) of the *r*-value of the DPH probe against temperature. Although for both pH solutions the anisotropy decreases with temperature, the anisotropy values are high even at 60 °C, suggesting the existence of a bilayer structure beyond physiological temperature. The decrease of *r*-value in the studied temperature range can be attributed to the gel-to-liquid-crystal phase transition of the lipid bilayer membranes. The phase transition temperatures for the SOBH-Chol mixture were obtained from the inflection point of the plots. T_m values of *ca.* 37 °C were obtained for vesicle solutions at both pH 8.0 and 12.0. This suggests that the packing of hydrocarbon chains of the bilayer become less rigid and thus can enhance the leaking of encapsulated drug molecules, if any. In other words, the prepared vesicles may be used as temperature-responsive drug delivery vehicles.

Upon addition of the Chol in the lipid matrix, the Chol molecules are incorporated into the bilayer resulting in a greater headgroup separation between the lipid monomers. Consequently, incorporation of Chol into lipids offers the vesicles a greater stabilization as a result of the minimization of headgroup-headgroup repulsions relative to that present in pure surfactant assemblies. Such stabilization can protect the vesicular structure from external physical factors, such as pH and salt (NaCl). We also found that with increasing NaCl concentration the fluorescence anisotropy exhibits very little change (Fig. 12(b)). High anisotropy value in the presence of 200 mM NaCl suggests that the vesicles formed with SOBH-Chol mixture are more stable than those formed by SOBH only. Similarly, keeping the molar concentration of the SOBH-Chol mixture fixed the solution pH was varied in the range 8–12. However, no significant change in *r*-value was observed with the decrease of pH (results are not shown here), indicating higher pH-stability. This is different from the results obtained in the absence of Chol (Fig. 3). In the absence of Chol, however, more changes in *r*-value were observed. This indicates that pH-induced leaking of encapsulated drug can be reduced by adding Chol.

Conclusions

In summary, we have synthesized a new surfactant, SOBH, which has very low CAC and γ_{CAC} values and acts as a very good surface-active agent. The results of surface tension, conductivity, fluorescence, DLS and TEM studies have shown the formation of vesicular structures by the zwitterionic and anionic forms of SOBH in the pH range 8–12. The vesicles formed by SOBH have hydrodynamic diameters in the range of 30–200 nm in pH 8 which increased to 60–300 nm in pH 12. In fact, depending upon the concentration of SOBH, the pH of the medium and the presence of salt or cholesterol gives different morphologies of the organized self-assemblies, for example small spherical vesicles and ribbons were observed which was suggested by the anisotropy (r) values of the DPH probe, and TEM and optical micrographs. The spherical vesicles are abundant in dilute alkaline solutions whereas other bilayer structures are predominantly present in relatively concentrated solutions and higher pH. The fluorescence probe studies indicate that the microenvironment of the self-assemblies is nonpolar and is very viscous, indicating rigid bilayer membranes, but they are capable of encapsulating polar molecules ,which was suggested by a conductivity experiment using KCl in the presence of SOBH. The vesicles produced in pH 8 solution are more stable than those formed in pH 12. The presence of cholesterol increases the rigidity and offers stability to the bilayer structures due to hydrophobic association with the alkyl chain of the amphiphile. The studies indicated that the vesicles obtained from pure SOBH and SOBH-Chol mixture can have potential applications in salt- and temperature-induced sustained release of drugs.

Acknowledgements

The authors gratefully acknowledge financial support for the work (Grant No.SR/S1/PC-18/2005) from the Department of Science and Technology, New Delhi. TP thanks CSIR (9/81(594)/2006-EMR-I) for a research fellowship. The authors thank Dr N. Chattopadhyay, Jadavpur University, Kolkata for his assistance with the fluorescence lifetime measurements.

References

1 C. F. van Nostrum, *Adv. Drug Delivery Rev.*, 2004, **56**, 9–16.
2 E. S. Lee, H. J Shin, K. Na and Y. H. Bae, *J. Controlled Release*, 2003, **90**, 363–374.
3 A. Mohanty, T. Patra and J. Dey, *J. Phys. Chem. B*, 2007, **111**, 7155–7159.
4 C. Tondre and C. Caillet, *Adv. Colloid Interface Sci.*, 2001, **93**, 115–134.
5 L. A. Estroff and A. D. Hamilton, *Chem. Rev.*, 2004, **104**, 1201–1218.
6 I. W. Hamley, *Angew. Chem., Int. Ed.*, 2003, **42**, 1692–1712.
7 G. Cevc, *Adv. Drug Delivery Rev.*, 2004, **56**, 675–711.
8 D. C. Drummond, M. Zignani and J. C. Leroux, *Prog. Lipid Res.*, 2000, **39**, 409–460.
9 S. Capone, P. Walde, D. Seebach, T. Ishikawa and R. Caputo, *Chem. Biodiversity*, 2008, **5**, 16–30.
10 C. Wang, Q. Gao and J. Huang, *Langmuir*, 2003, **19**, 3757–3761.
11 C. Wang, J. Huang, S. Tang and B. Zhu, *Langmuir*, 2001, **17**, 6389–6392.
12 W. J. Chen, G. Z. Li, G. W. Zhou, L. M. Zhai and Z. M. Li, *Chem. Phys. Lett.*, 2003, **374**, 482–486.
13 M. Scarzello, J. E. Klijn, A. Wagenaar, M. C. A. Stuart, R. Hulst and J. B. F. N. Engberts, *Langmuir*, 2006, **22**, 2558–2568.
14 K. Edwards, M. Silvander and G. Karlsson, *Langmuir*, 1995, **11**, 2429–2434.
15 H. Kawasaki, M. Souda, S. Tanaka, N. Nemoto, G. Karlsson, M. Almgren and H. Maeda, *J. Phys. Chem. B*, 2002, **106**, 1524–1527.
16 R. Cazzola, P. Viani, P. Allevi, G. Cighetti and B. Cestaro, *Biochim. Biophys. Acta, Biomembr.*, 1997, **1329**, 291–301.
17 M. B. Yatvin, W. Kreutz, B. A. Horowitz and M. Shinitzky, *Science*, 1980, **210**, 1253–1255.
18 L. Di. Marzio, C. Marianecci, B. Cinque, M. Nazzarri, A. M. Cimini, L. Cristiano, M. G. Cifone, F. Alhaique and M. Carafa, *Biochim. Biophys. Acta, Biomembr.*, 2008, **1778**, 2749–2756.
19 L. Jiang, K. Wang, F. Ke, D. Liang and J. Huang, *Soft Matter*, 2009, **5**, 599–606.
20 D. C. Litzinger and L. Huang, *Biochim. Biophys. Acta, Rev. Biomembr.*, 1992, **1113**, 201–227.
21 H. Jizomoto, E. Kanaoka and K. Hirano, *Biochim. Biophys. Acta, Lipids Lipid Metab.*, 1994, **1213**, 343–348.
22 M. H. Chung, Y. C. Chung and B. C. Chun, *Colloids Surf., B*, 2003, **29**, 75–80.
23 N. Nishikawa, M. Arai, M. Ono and I. Itoh, *Langmuir*, 1995, **11**, 3633–3635.
24 M. Bergsma, M. L. Fielden and J. B. F. N. Engberts, *J. Colloid Interface Sci.*, 2001, **243**, 491–495.
25 M. Johnsson, A. Wagenaar and J. B. F. N. Engberts, *J. Am. Chem. Soc.*, 2003, **125**, 757–760.
26 M. Carafa, L. Di Marzio, C. Marianecci, B. Cinque, G. Lucania, K. Kajiwara, M. G. Cifone and E. Santucci, *Eur. J. Pharm. Sci.*, 2006, **28**, 385–393.
27 Y. Sumida, A. Masuyama, M. Takasu, T. Kida, Y. Nakatsuji, I. Ikeda and M. Nojima, *Langmuir*, 2001, **17**, 609–612.
28 D. Collins, D. C. Litzinger and L. Huang, *Biochim. Biophys. Acta, Biomembr.*, 1990, **1025**, 234–242.
29 M. L. Fielden, C. Perrin, A. Kremer, M. Bergsma, M. C. Stuart, P. Camilleri and J. B. F. N. Engberts, *Eur. J. Biochem.*, 2001, **268**, 1269–1279.
30 P. C. Bell, M. Bergsma, I. P. Dolbnya, W. Bras, M. C. A. Stuart, A. E. Rowan, M. C. Feiters and J. B. F. N. Engberts, *J. Am. Chem. Soc.*, 2003, **125**, 1551–1558.
31 L. Wasungu, M. Scarzello, G. van Dam, G. Molema, A. Wagenaar, J. B. F. N. Engberts and D. Hoekstra, *J. Mol. Med.*, 2006, **84**, 774–784.
32 M. B. Dowling, J. Ho Lee and S. R. Raghavan, *Langmuir*, 2009, **25**, 8519–8525.
33 G. D. Smith and R. E. Barden, *Chem. Phys. Lipids*, 1975, **14**, 1–14.
34 P. P. Karmali, B. K. Majeti, B. Sreedhar and A. Chaudhuri, *Bioconjugate Chem.*, 2006, **17**, 159–171.
35 S. Franceschi, N. de Viguerie, M. Riviere and A. Lattes, *New J. Chem.*, 1999, **23**, 447–452.
36 G. K. Ragunathan and S. Bhattacharya, *Chem. Phys. Lipids*, 1995, **77**, 13–23.
37 K. Ohkubo, K. Sugahara, H. Ohta, K. Tokuda and R. Ueoka, *Bull. Chem. Soc. Jpn.*, 1981, **54**, 576–578.
38 H. Murase, A. Nagao and J. Terao, *J. Agric. Food Chem.*, 1993, **41**, 1601–1604.
39 T. Patra, A. Pal and J. Dey, *Langmuir*, 2010, **26**, 7761–7767.
40 A. Mohanty and J. Dey, *Langmuir*, 2004, **20**, 8452–8459.
41 A. Mohanty and J. Dey, *Chem. Commun.*, 2003, (12), 1384–1385.
42 A. Mohanty and J. Dey, *Langmuir*, 2007, **23**, 1033–1040.
43 S. Bhattacharya, M. Subramanian and U. S. Hiremath, *Chem. Phys. Lipids*, 1995, **78**, 177–188.
44 D. E. Koppel, *J. Chem. Phys.*, 1972, **57**, 4814–4820.
45 C. D. Hodgman, R. C. weast, S. M. Selby, *Hand book of Chemistry and Physics*, 4th ed.; Chemical Rubber Publishing Co.; Cleveland, Ohio, 1958.
46 (*a*) H. Maeda and R. Kakehashi, *Adv. Colloid Interface Sci.*, 2000, **88**, 275–293; (*b*) N. Kashima, S. Yamanaka, K. Mitsugi and Y. Hirose, *Agric. Biol. Chem.*, 1976, **40**, 41–47.
47 M. J. Rosen, *Surfactants and Interfacial Phenomena*, 4th edn, Wiley-Interscience, New York, 2004.
48 E. M. Varka, E. Coutouli-Argyropoulou, M. R. Infante and S. Pegiadou, *J. Surfactants Deterg.*, 2004, **7**, 409–414.
49 J. N. Israelachvili, *Intermolecular and Surface Forces*, 2nd edn, Academic Press, New York, 1991.
50 G. Basu Ray, S. Ghosh and S. P. Moulik, *J. Surfactants Deterg.*, 2009, **12**, 131–143.
51 J. T. Edward, *J. Chem. Educ.*, 1970, **47**, 261–270.

52 (*a*) M. Shinitzky and Y. Barenholz, *J. Biol. Chem.*, 1974, **249**, 2652–2657; (*b*) M. Shinitzky, A. C. Dianoux, C. Itler and G. Weber, *Biochemistry*, 1971, **10**, 2106–2113; (*c*) M. Shinitzky and I. Yuli, *Chem. Phys. Lipids*, 1982, **30**, 261–282.
53 S. Roy and J. Dey, *Langmuir*, 2005, **21**, 10362–10369.
54 P. Debye, *Polar Molecules*, Dover, New York, 1929.
55 J. R. Lakowicz, *Principles of Fluorescence Spectroscopy*, Plenum Press, New York, 1983, p. 132.
56 S. Roy, A. Mohanty and J. Dey, *Chem. Phys. Lett.*, 2005, **414**, 23–27.
57 K. Kalyanasundaram and J. K. Thomas, *J. Am. Chem. Soc.*, 1977, **99**, 2039–2044.
58 (*a*) K. Kalyansundaram, *Photophysics of Microheterogeneous Systems*; Academic Press, New York, 1988; (*b*) J. K. Thomas, *The Chemistry of Excitation at Interfaces*; ACS Monograph 181, American Chemical Society, Washington DC, 1984; (*c*) F. M. Winnik and S. T. A. Regismond, *Colloids Surf., A*, 1996, **118**, 1–39.
59 K. Morigaki and P. Walde, *Curr. Opin. Colloid Interface Sci.*, 2007, **12**, 75–80.
60 B. Vijai. Shankar and A. Patnaik, *Langmuir*, 2007, **23**, 3523–3529.
61 A. Ghosh and J. Dey, *J. Phys. Chem. B*, 2008, **112**, 6629–6635.
62 A. Ghosh and J. Dey, *Langmuir*, 2008, **24**, 6018–6026.
63 M. Singh, M. K. Trivedi and J. Bellare, *J. Mater. Sci.*, 1999, **34**, 5315–5323.
64 D. A. Jaeger and E. L. G. Brown, *Langmuir*, 1996, **12**, 1976–1980.
65 G. Szabo, *Nature*, 1974, **252**, 47–49.
66 C. R. Loomis, G. G. Shipley and D. M. Small, *J. Lipid Res.*, 1979, **20**, 525–535.
67 J. Y. Huang, J. T. Buboltz and G. W. Feigenson, *Biochim. Biophys. Acta, Biomembr.*, 1999, **1417**, 89–100.
68 (*a*) V. Pata and N. Dan, *Biophys. J.*, 2005, **88**, 916–924; (*b*) C. R. Benatti, M. T. Lamy and R. M. Epand, *Biochim. Biophys. Acta, Biomembr.*, 2008, **1778**, 844–853.
69 M. B. Sankaran and T. E. Thompson, *Biochemistry*, 1990, **29**, 10676–10684.
70 S. Bhattacharya and S. Halder, *Biochim. Biophys. Acta, Biomembr.*, 1996, **1283**, 21–30.